Appl. Phys. B 69, 61–70 (1999) / Digital Object Identifier (DOI) 10.1007/s003409900024

Applied Physics B
Lasers
and Optics

Rate-equation modeling of single- and multiple-quantum vibrational energy transfer of OH ($A^2\Sigma^+$, $v' = 0$ to 3)

U. Rahmann, W. Kreutner, K. Kohse-Höinghaus

Universität Bielefeld, Fakultät für Chemie, Physikalische Chemie 1, D-33615 Bielefeld, Universitätsstraße 25, Germany
(Fax: +49-521/106-6027, E-mail: kkh@pc1.chemie.uni-bielefeld.de)

Received: 25 August 1998/Revised version: 22 December 1998/Published online: 28 April 1999

Abstract. A computer code based on a kinetic rate-equation model for describing the collisional dynamics of OH ($A^2\Sigma^+$) in laser-induced fluorescence experiments was developed. In this work, the capabilities of the simulation code are extended to include the vibrational states up to the OH ($A^2\Sigma^+$, $v' = 3$) level. The calculation of quenching, rotational and vibrational relaxation rate coefficients for different collider species is discussed. Problems that arise for the description of vibrational relaxation include the branching ratio between single- and multiple-quantum steps and the form of the nascent rotational distribution after a vibrational relaxation step. Experimental spectra recorded under a variety of conditions are simulated using a consistent set of model assumptions. The calculations must include vibrational relaxation steps up to $\Delta v = 3$ to account for the experimental intensity distributions. Effects due to polarized laser excitation become more important for vibrational states with $v' > 1$. Areas for future work are identified, including determination of experimental rate coefficients for state-changing and depolarizing collisions in the upper vibrational levels.

PACS: 34.50.Ez; 82.40.Py

The OH radical is one of the key species in the kinetics of both combustion and atmospheric chemistry. A large amount of work has been spent in developing measurement methods for this reaction intermediate, and laser-induced fluorescence (LIF) is now perhaps the most popular tool for the detection of OH. In the combustion field, the applications [1–5] of OH LIF range from pointwise concentration measurement in small laminar flames to two-dimensional, single-shot temperature determination in turbulent, reacting flows, and from low-pressure flames in the laboratory to the high-pressure, high-temperature environment in the cylinder of a running internal combustion engine. Depending on the application, various experimental configurations may be used. One degree of freedom is the choice of the laser-pumped vibrational level in the OH ($A^2\Sigma^+$) state; different excitation schemes involving the levels up to $v' = 3$ are typically employed.

The LIF signal is influenced by a number of collision processes in the excited state which compete with emission: electronic quenching, rotational and vibrational relaxation change the population distribution and modify the spectral and temporal shape of the signal. Additionally, the higher rovibrational levels of the OH $A^2\Sigma^+$ state are predissociative, which provides a non-collisional removal channel that competes with emission. If the intensity of the excitation laser is high enough to significantly perturb the population in the lower laser-coupled level, relaxation in the electronic ground state will also play a role. An important aspect during LIF method development has therefore been the numerical simulation of the various radiative and collisional processes. With the aid of model calculations the importance of experimental parameters and their influence on the LIF signal may be estimated or even quantified under the particular conditions of a specific measurement situation. Simulations allow one to make a well-informed choice between different available measurement strategies; a typical example would be an optimization of the spectral or temporal detection interval. Also, sources of systematic errors may be discovered which cannot be discerned by just inspecting the experimental raw data.

One of the key issues in the development of LIF simulation models has been the inclusion of these collisional processes. As more experimental and theoretical data become available, the models (see for example [6–8]) can be refined to describe in increasing detail the dynamics of the levels that are involved. In previous work [9, 10], a model code (called LASKIN) was described which simulates the population dynamics in the OH $A^2\Sigma^+$ ($v' = 0$ and 1) state for the case of linear excitation LIF. For the investigations described in this paper, two higher vibrational levels ($v' = 2$ and 3) were included in this code. Excitation to the $v' = 3$ level was suggested [11] as a means for circumventing problems in the LIF data analysis caused by poorly known collisional relaxation processes. The examination of this excitation scheme was the main goal in the extension of the LASKIN code. The introduction of the appropriate rate coefficients, and in particular some specific aspects concerning vibrational relaxation from levels $v' > 1$ are discussed. The extended code was tested in the simulation of some experimental spectra.

1 Simulation approach

After excitation into a specific rovibrational level of the OH $A^2\Sigma^+$ state, spontaneous emission competes with bath gas collisions, which may transfer the molecule to a different rotational state within the same vibrational manifold (rotational energy transfer, RET), or to a different vibrational level (vibrational energy transfer, VET). These collisions lead to the appearance of additional rotational lines (RET) and new vibrational bands (VET) in the emission spectrum. Another possible result of a collision is electronic quenching, which will reduce the overall signal intensity. In the case of the OH $A^2\Sigma^+$ state, and under typical flame conditions, all three types of inelastic collisions must be taken into account, because they occur on roughly comparable time scales. Their relative probabilities depend on temperature, the chemical nature and number densities of collision partners, and the rovibrational state considered. The OH molecule may (and in most flames will) experience more than one inelastic collision before emission, and the observable signal is then the net result of several competing processes. For the higher vibrational levels of OH $A^2\Sigma^+$, predissociation is an intrinsic loss mechanism which does not depend on external parameters, but shows a marked dependence on quantum state [12, 13]. Elastic, depolarizing collisions also play a role for interpreting LIF measurements [14–16]; their detailed treatment, however, is beyond the scope of this paper.

In several publications, measurement procedures employing excitation to the predissociating $v' = 2$ [17, 18] and $v' = 3$ [11, 19–23] levels of the OH ($A^2\Sigma^+$) state were described. These experimental approaches are less susceptible to relaxation processes because of the short predissociative lifetimes. However, as was already shown in [11], collisions are not completely negligible at atmospheric pressure. Signals from collision-populated vibrational levels may even dominate the observable spectrum [24]. Therefore it seems desirable to assess the effects of collisions for the $v' = 2$ and $v' = 3$ levels. Quantitative information on collisional processes in these levels is, however, extremely sparse.

The LASKIN code was developed and tested using data and spectra of the lower vibrational states, $v' = 0$ and $v' = 1$. It can reasonably well reproduce experimental spectra taken under a wide range of conditions of pressure, temperature, and composition. Hence an attempt is made here to expand the simulation code to include the next two higher vibrational levels. The rate coefficients required to describe these levels must be largely estimated; previous experience with the lower levels provides a good starting point for this task. The present simulations may then be compared with some experimental spectra available from the literature. Although it is clear from the start that no perfect match will be achievable in this manner, some trends for the behaviour in these higher vibrational levels become discernible.

In the LASKIN code [9], the temporal evolution of level populations is modeled using coupled rate equations for the individual rotational states and a time-dependent laser excitation function. It is assumed that the laser intensity is in the regime of linear excitation where the population in the lower laser-coupled level is not perturbed. The electronic ground state can therefore be simplified to contain only two levels which are not coupled to one another: One level is the lower laser-coupled state; the second acts as target level for all spontaneous emission and quenching processes. In order to reduce the computational task, the range of rotational levels considered in the excited electronic state is restricted to $N' \leq 20$. This means that at 3000 K more than 95% of all molecules will still be included in the calculation. To minimize the size of the differential equation system, only downward vibrational relaxation is taken into account. This is obviously not perfectly correct, since it negates microscopic reversibility. Some problems were encountered, in particular with respect to multiquantum VET to all accessible rovibrational states; together with technical limitations this prevented so far the full implementation of detailed balance in the code. However, a test case was calculated for the $v' = 1 \rightarrow 0$ transition at 2250 K, comparing the resulting spectra (0–0 and 1–1 band) with and without inclusion of detailed balancing. It was found that the differences in the resulting spectra were barely distinguishable. The ratio of signal amplitudes deviated from unity by less than 5% (1% on average), and this error is likely to further decrease with increasing Δv.

Following [9], the time-dependent population of a collision-populated rotational level j is described by (1):

$$\frac{\mathrm{d}n_j}{\mathrm{d}t} = \left(\sum_{i \neq j} R_{ij} n_i + \sum_{i \neq j} V_{ij} n_i \right) - n_j \times \left(\sum_{i \neq j} R_{ji} + \sum_{i \neq j} V_{ji} + Q_j + A_j + P_j \right) . \quad (1)$$

Here, R_{ij} is the state-to-state rate for RET from initial level i to target level j; similarly, V_{ij} is the state-to-state VET rate; Q_j denotes the quenching rate for level j; and A_j and P_j are the Einstein A coefficients for spontaneous emission and the predissociation rate, respectively. The sums are taken over all levels in the excited state. (The equations for the laser-coupled levels contain additional terms to account for absorption, stimulated emission, and laser pulse time dependence, see [9]). It should be noted that, by definition, R_{ij} will be zero for all levels j that do *not* belong to the same vibrational manifold as level i. The reverse is true for V_{ij}. In a flame, usually more than one collider species contributes; under particular conditions in low-pressure flames, even unstable species such as H atoms may be present in quite appreciable concentrations [25]. The collisional rates in (1) are already a weighted average over the contributions of all the collider species present in the flame:

$$V_{ij} = \sum_{\mathrm{M}} n_{\mathrm{M}} k_{ij}^{v}(\mathrm{M}) . \quad (2)$$

Here, n_{M} is the number density and $k_{ij}^{v}(\mathrm{M})$ the second-order VET rate coefficient for collider M; similar equations hold for the other energy transfer rates in (1).

In flames, the number of rotational levels that must be considered is large, even in the simplest case when only the lowest vibrational state ($A^2\Sigma^+$ $v' = 0$) is populated. If one of the higher vibrational states is initially laser-pumped, relaxation will further increase the number of levels involved. Hence, a vast number of temperature-dependent, collider-specific, state-to-state rate coefficients must be available as an input to the calculation. In fact, the number of coefficients

required is much larger than even the most ambitious experimental project could ever hope to provide. Therefore other sources are called for. One approach to this problem (see [26] and literature cited therein) makes use of scaling relationships, for example the "Energy Corrected Sudden" or ECS law [27], which allow the calculation of a complete array of state-to-state RET coefficients from a relatively small set of so-called basis coefficients. These may in turn be the result of a quantum mechanical calculation, or may be determined experimentally. This approach works very well for H_2O; for N_2 and CO_2 the situation is not quite as satisfactory, but comparison with experimental spectra shows that good agreement can be achieved [9, 10, 28].

Quenching coefficients for $v' = 0$ and 1 were determined experimentally for a fairly large range of quantum states, temperatures, and colliders, and very reasonable results are obtained when interpolating and extrapolating the trends found from such measurements. A large compilation of experimental data can be found in [29]; comparison is made there to calculations based on the "harpooning" mechanism. Using these results, species-specific OH quenching coefficients may be calculated for a wide range of colliders and temperatures that occur in flames.

Tables 1a and 1b summarize the assumptions used for the calculation of quenching, VET and RET coefficients for the major colliders encountered in the flames that were simulated here. The temperature behaviour of quenching and VET was approximated with a $\sqrt{T/T_0}$ dependence, where T_0 is the reference temperature given in the last column of Table 1a. In Table 1b, the quantities C, α, β, and l_c are fitting parameters used in the calculation of RET coefficients [26].

2 Results

2.1 Extensions to the code

Compared with the state of development described in [9, 10], progress was made by including the vibrational levels $v' = 2$ and $v' = 3$ in the differential equation system.

The number of rovibrational levels that must be taken into account has almost doubled, and the differential equation solver [30] employed in the code had to be adapted to this task. The necessary Einstein A and B coefficients were taken from the LIFBASE database [31]. Predissociation rates were obtained from the same reference [31]; for rotational levels in $v' = 3$ with $N' > 15$, an interpolating curve was fitted to the theoretical values of Yarkony [32]. A new target level for the predissociated molecules was introduced. This was preferred over assigning the predissociation channel to

Table 1a. Rate coefficients for total VET ($k_i^{\text{VET, total}}$ for $v' = 1 \rightarrow 0$; see (3)) and quenching (k_Q), and their dependence on rotational ($f(N')$) and vibrational ($f(v')$) state and temperature ($f(T)$), as assumed for the LASKIN calculations reported here

Collider	$k_i^{\text{VET, total}}$ $(v' = 1 \rightarrow 0,\ N' = 0,\ T_0)$ $(/1 \times 10^{-10}\ \text{cm}^3\ \text{s}^{-1})$	k_Q $(v' = 0,\ N' = 0,\ T_0)$ $(/1 \times 10^{-10}\ \text{cm}^3\ \text{s}^{-1})$	T_0/K
H_2O	0.127	7.610	1600
N_2	0.910	0.153	1600
CO_2	1.333	1.611	2250
CO	1.231	1.231	2250
H_2	3.33	2.113	1600
O_2	2.028	1.444	1600
H	10.1	9.04	1600
He	0	0	–
$f(T)$	$k(T) \sim \sqrt{(T/T_0)}$	$k(T) \sim \sqrt{(T/T_0)}$	
$f(N')$	$k(N') = k(0) \times (1 - 0.0343 \times N')$	$k(N') = k(0) \times \exp(-a(T) \times N')$	
		$T = 300$ K $\quad a(T) = 0.0395$	
		$T = 1200$ K $\quad a(T) = 0.02$	
		$T = 1700$ K $\quad a(T) = 0.012$	
		$T = 1900$ K $\quad a(T) = 0.007$	
		$T \geq 2300$ K $\quad a(T) = 0.0$	
$f(v')$	$k(v' = e \rightarrow\ f) = k(v' = 1 \rightarrow 0)$	$k(v' = 1) = 0.85 \times k(v' = 0)$	
		$k(v' = 2) = 0.70 \times k(v' = 0)$	
		$k(v' = 3) = 0.60 \times k(v' = 0)$	

Table 1b. Parameters for the calculation of basis coefficients and state-to-state RET coefficients as used in the simulations reported here. C, α, and β are fitting parameters to describe the basis coefficients; l_c is an interaction length; E_N is the rotational energy of level N'. The ECS scaling law was applied as described in (2)–(5) and (9) of [26]. It should be noted that (9) for the calculation of basis coefficients $k_{\text{F1}(N) \rightarrow \text{F1}(0)}$ was slightly modified for this work. The RET coefficients were assumed to be identical for all vibrational states. Temperature dependence is implicitly accounted for by the scaling law

Scaling of basis coefficients: $k_{\text{F1}(N) \rightarrow \text{F1}(0)} = C \times E_N^{-\alpha} \times \exp(-\beta E_N / kT)$							
Collider	$C/1 \times 10^{-10}\ \text{cm}^3\ \text{s}^{-1}$				α	β	l_c/
	$T = 300$ K	2050 K	2250 K	2500 K			Å
H_2O	–	345	355	370	1.3	0	0.7
N_2	23.8	34.5	35.5	37	1.1	0	0.9
CO_2	–	34.5	35.5	37	1.1	0	0.9
CO	–	34.5	35.5	37	1.1	0	0.9
He ($\Delta N'$even)	387	–	–	–	1.52	0.63	3.33
He ($\Delta N'$odd)	0.0294	–	–	–	0	0.865	3.33

the same target level as quenching. In this way, bookkeeping will be facilitated when saturation effects and depletion of the ground state [33, 34] are incorporated. To the best of our knowledge, no state-specific quenching rate coefficients were directly measured so far for $v' > 1$. Paul [29] suggests that quenching cross sections may increase for the higher vibrational states. However, the experiments in [10] resulted in a slightly reduced quenching coefficient for $v' = 1$. Therefore we decided to extrapolate the experimentally observed trend to the higher levels; i.e. for a given rotational quantum number, the quenching rate coefficients for higher vibrational states were scaled with 0.85 ($v' = 1$), 0.70 ($v' = 2$), and 0.60 ($v' = 3$) of the value that was calculated for $v' = 0$ (see Table 1a).

Regarding the RET coefficients, again no state-to-state measurements have been reported for $v' > 1$. In the simulations described in this work, the rotational relaxation coefficients were assumed to be independent of v' and identical with those for $v' = 0$. This decision was made based on the observations of [35] who, within experimental error, found the same room temperature state-to-state RET coefficients in $v' = 1$ as in $v' = 0$. Very recently, total RET cross sections for $v' = 2$ were reported [18] from flame measurements; they exhibit the same trend. Also, RET rates [36] for collisions with O_2 in the $X\,^2\Pi$ ground state of OH did not exhibit a marked dependence on vibrational level.

2.1.1 Problems specific to VET. It should be noted that the VET coefficients used in (2) are written as state-to-state-specific quantities, i.e. the rovibrational quantum numbers of both *initial and target levels* are presumed to be known. This is not yet the case. The finest level of experimental detail obtained so far [10, 37] for high-temperature conditions was measurement of a collider-specific (collider $M = H_2O$, N_2) rate coefficient for the $v' = 1 \rightarrow 0$ transition, which is also specific in terms of the initially pumped OH rovibrational level ($N' = 1$, 5, and 13 in $v' = 1$); rotational resolution of the target levels in the VET process was not achieved. In terms of (2), the quantity measured in [10] was

$$k_i^{\text{VET, total}}(\text{M}) = \sum_j k_{ij}^v(\text{M}) \,, \tag{3}$$

i.e. a total downward VET rate coefficient for a particular initially pumped rotational level $i = N'$ in $v' = 1$ (where j encompasses all rotational levels in the target vibrational manifold $v' = 0$).

Therefore several problems must be addressed for the modeling of VET. Total VET rate coefficients are available for the $v' = 1 \rightarrow v' = 0$ relaxation step, for a very limited number of collider species and rotational levels. Some interpolation and extrapolation scheme must be applied to provide the full set of total VET coefficients for $v' = 1$ (see Table 1a). Next, these total VET coefficients $k_i^{\text{VET, total}}$ have to be decomposed into the state-to-state coefficients k_{ij}^v required for (2); this choice will determine the shape of the nascent rotational distribution in the collision-populated state. Finally, if the $v' = 2$ or $v' = 3$ states are excited, additional assumptions have to be made about their behaviour. Vibrational relaxation towards $v' = 1$ and 0 may proceed as a sequence of steps (with $\Delta v = 1$ for each step) or in a single-step fashion (with $\Delta v = 2$ or 3 also occurring). The question is then, which mechanisms actually occur, and what their relative probabilities are.

Obviously, some theoretical guidance would be beneficial for these tasks. However, for systems involving free radicals like OH little seems to be known so far that could provide a practicable rule for describing the VET step and in particular its dependence on rotational quantum states and collider species. As a preliminary working solution for the problem, a very simple approach was adopted in [10] to estimate state-to-state-specific rate coefficients k_{ij}^v from the experimentally available total VET rates. Briefly, it was assumed (see Fig. 8 in [10] and the associated text there) that only downward, exoergic transitions occur. For the J-scaling of the rate coefficients, several model assumptions were evaluated; two of them were relatively successful in reproducing the rotational distributions that were observed experimentally. The first of these assumptions is that the VET rate coefficients, which link a particular initial rotational level in $v' = 1$ to the levels in $v' = 0$, are equal for all target rotational quantum numbers ("equal probability" model). The second assumption is that the VET rate coefficients are proportional to $(2J_{\text{target}} + 1)$, thus taking into account rotational degeneracies ("$2J + 1$" model). Note that both models lead to broad rotational distributions in the collision-populated vibrational states. The RET within the target state will, of course, rapidly modify this nascent distribution. These model assumptions were motivated by VET experiments both at room temperature and in flames, where rotational distributions were observed in the collision-populated state which gave a "hot" spectrum, with apparent "temperatures" much higher than the bath gas [10, 38, 39]. In [39] the influence of different collider species on this rotational distribution was investigated at room temperature. One other model for the transition rates which was also tested in [10] assumes complete conservation of the rotational quantum number J, but does not seem to give a good description for the OH system.

2.2 Simulation of RET

The now extended LASKIN code was first applied to LIF spectra of the OH 2–1 band [18] and 3–2 band [11]. The primary purpose here was to check the assumptions made for the RET coefficients in the upper vibrational levels. The 2–1 band spectra were measured in an atmospheric pressure methane–oxygen flame after excitation of the $P_1(12)$ line of the 2–0 band with a pulse of approximately 700 ps duration; the signal was detected with a temporal gate of about 400 ps. As described in [18], the spectra were processed to remove laser polarization effects; the flame temperature was measured to be 3010 K. For the 3–2 band spectra, OH was produced in an atmospheric pressure hydrogen–oxygen flame and was excited with an excimer laser pulse, using the 3–0 band $Q_2(11)$ line. The signal was temporally integrated. For further experimental details see [11, 18].

Figures 1a and 1b compare LASKIN simulations with two measured 2–1 band spectra (the experimental data sets are identical with those of Fig. 2 in [18]). The LIF signal was detected at two instants during and after the excitation pulse (nominally at a delay of $\Delta t = -0.5$ ns and $\Delta t = +1.50$ ns, relative to the pulse peak). The number of populated levels increases rapidly. At short times, the number and intensity

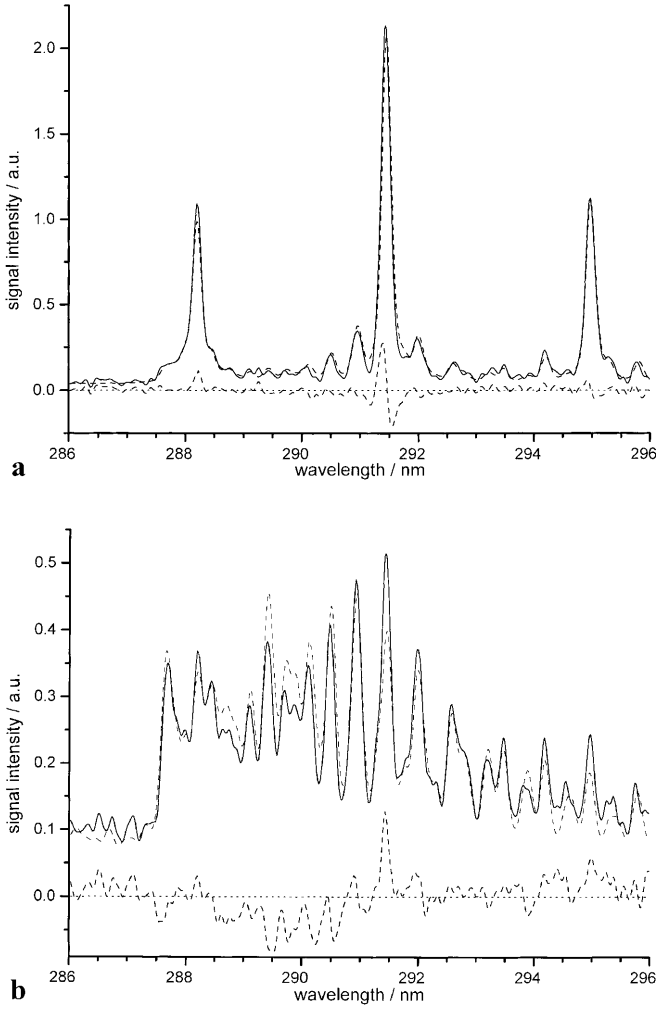

Fig. 1a,b. Experimental OH LIF spectra [18] and simulation. *Full line*: spectra measured in an atmospheric pressure CH_4/O_2 flame. Laser pulse with 700 ps effective width. Excitation: 2–0 band, $P_{11}(12)$ line. Detection: 2–1 band, using a 400 ps wide temporal gate. *Broken line*: simulation using the LASKIN code. *Lower curve*: difference (measurement – simulation). **a** The detection gate was set at nominally $\Delta t = -0.5$ ns before the peak of the laser pulse. **b** The gate was set at nominally $\Delta t = +1.5$ ns after the peak of laser pulse. The figures may be compared directly with Fig. 2 in [18]

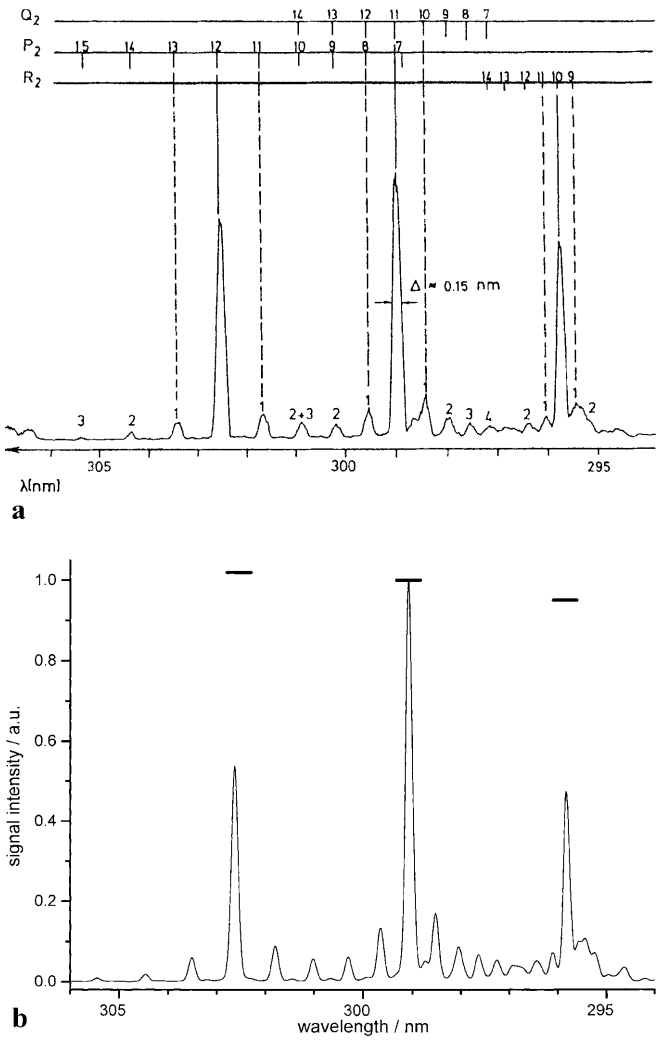

Fig. 2a,b. Experimental OH LIF spectrum [11] and simulation. **a** Spectrum measured in an atmospheric pressure H_2/O_2 flame. Excitation: 3–0 band, $Q_2(11)$ line. Detection: 3–2 band, temporally integrated signal. **b** Simulation using the LASKIN code. The reduced number of rotational lines as compared with Fig. 1b should be noted. Signal intensities of the curve in **b** correspond to the Einstein A coefficients. *Horizontal bars* above the three prominent P-, Q-, and R-branch lines correspond to signal amplitudes calculated for the "collision-free" case [14] after excitation with linearly polarized laser light

of lines from collision-populated levels is well reproduced by the simulation in Fig. 1a. In Fig. 1b, the general shape of the spectrum is predicted quite well; however, some discrepancies are apparent in the intensity ratios between different lines. The DC offset which appears in Fig. 1b can be attributed in part to signal from the collisionally populated $v' = 1$ vibrational level, but partly also to an experimental artefact. Inspection of a series of spectra where the gate was shifted in 500 ps increments shows that the simulation works less satisfactory at the very beginning of the laser pulse and for times later than about 3 ns. A possible reason for these discrepancies, particularly at the beginning of the laser pulse, may be a difference between the temporal pulse shape employed in the simulation and the actual laser pulse. At late times, an inadequate assumption concerning the RET coefficients should become most readily visible. Also, the signal-to-noise ratio in these "late" spectra decreases.

In Fig. 2a, OH emission in the 3–2 band is shown [11] for a hydrogen–oxygen flame. For the simulation in Fig. 2b, the concentrations of collision partners and the temperature ($T = 2000$ K) had to be estimated; data of a similar flame [40] were used. The RET effects in the spectrum can be reproduced very well. It is obvious that the total number of lines in this spectrum is much smaller than in the $v' = 2$ case, even though the fluorescence signal was time-integrated. This is caused by the shorter predissociation lifetimes of the rotational levels on the order of 30–300 ps in the $v' = 3$ state which do not allow for many collisions. It is also obvious that the relative intensities of the three prominent lines (the P-, Q-, and R-branch lines originating from the laser-pumped level) are not well matched by the simulation. In the calculation, the line intensities are proportional to the corresponding Einstein A coefficients. Because polarized laser radiation was used for recording this spectrum, the detected signal intensities deviate from this simple proportionality [14]. In the particular case considered here (excitation of a Q-branch

line, detection under 90 degrees, laser polarization parallel to the plane of detection, both signal polarization components measured), the P- and R-branch lines are detected more efficiently, hence the experimental line intensities appear distorted. Depolarizing collisions will tend to establish a ratio of signal amplitudes according to the Einstein coefficients. Following [14], relative signal intensities were calculated for the case of an "aligned" sample, i.e. without depolarizing collisions. The horizontal bars above the P- and R-branch line positions in the simulation indicate these hypothetical signal amplitudes, relative to the Q-branch line. In the observed spectrum the situation seems to be somewhere intermediate between the collision-free case and the case corresponding to the Einstein A coefficients.

To summarize briefly: There still is a lack of experimental or theoretical data regarding collision processes in the higher vibrational states ($v' = 2$ and 3) of OH. In that situation, the use of RET rate coefficients that were derived for the $v' = 0$ state of OH seems to provide a reasonably good "first guess" for the description of the rotational relaxation behaviour in the upper vibrational states.

2.3 Simulation of VET

While signal from collision-populated vibrational levels was already described in the first paper [11] on LIF with excitation to $v' = 3$, many important details, and in particular the rate coefficients involved, are still unknown. Hence for a simulation of these signals several assumptions have to be made and tested by comparison with experimental spectra.

In [24, 40] a series of OH LIF spectra with excitation to $v' = 3$ was measured for a wide range of pressures and several combinations of fuel and oxidizer. Some of these spectra were used for comparison with the present simulations. An atmospheric pressure, premixed methane–oxygen flame ($T = 2250$ K; $\phi = 1.03$) was chosen as the first test case [40]. The main collider species in this flame are H_2O and CO_2. Water is known to be a fast quencher but rather slow at VET; CO_2 is approximately equally efficient in both processes, whereas nitrogen is a poor quencher, but efficient for VET [41]. Fluorescence was excited using the $Q_1(4)$ line of the 3–0 band, and a wide spectral range was scanned encompassing the progressions with $\Delta v = 0$ (3–3, 2–2, 1–1 and 0–0 band) and $\Delta v = 1$ (3–2, 2–1, and 1–0 band), respectively. The signal was temporally integrated.

The best simulation obtained for these experimental conditions is shown in Fig. 3a. Table 1 summarizes the assumptions made for calculating the coefficients. As discussed above, the RET coefficients were assumed to be the same for all vibrational levels involved, and quenching was assumed to show a decrease with v'. Vibrational relaxation was assumed to be permitted for all vibrational transitions, regardless of collider, Δv and initial state. For the transitions with $\Delta v = 1$, 2, or 3 arising from the $v' = 2$ and 3 states, the VET rate coefficients $k_i^{\text{VET, total}}$ were set identical to those that were measured and estimated for the $v' = 1 - 0$ transition (furthermore, the "equal probability" model described above was used to estimate the k_{ij}^{v} coefficients). The experimental slit function (nominally 0.8 nm resolution) was modeled as a Voigt profile. Due to laser polarization effects, signal intensities are again distorted for the lines originating from the

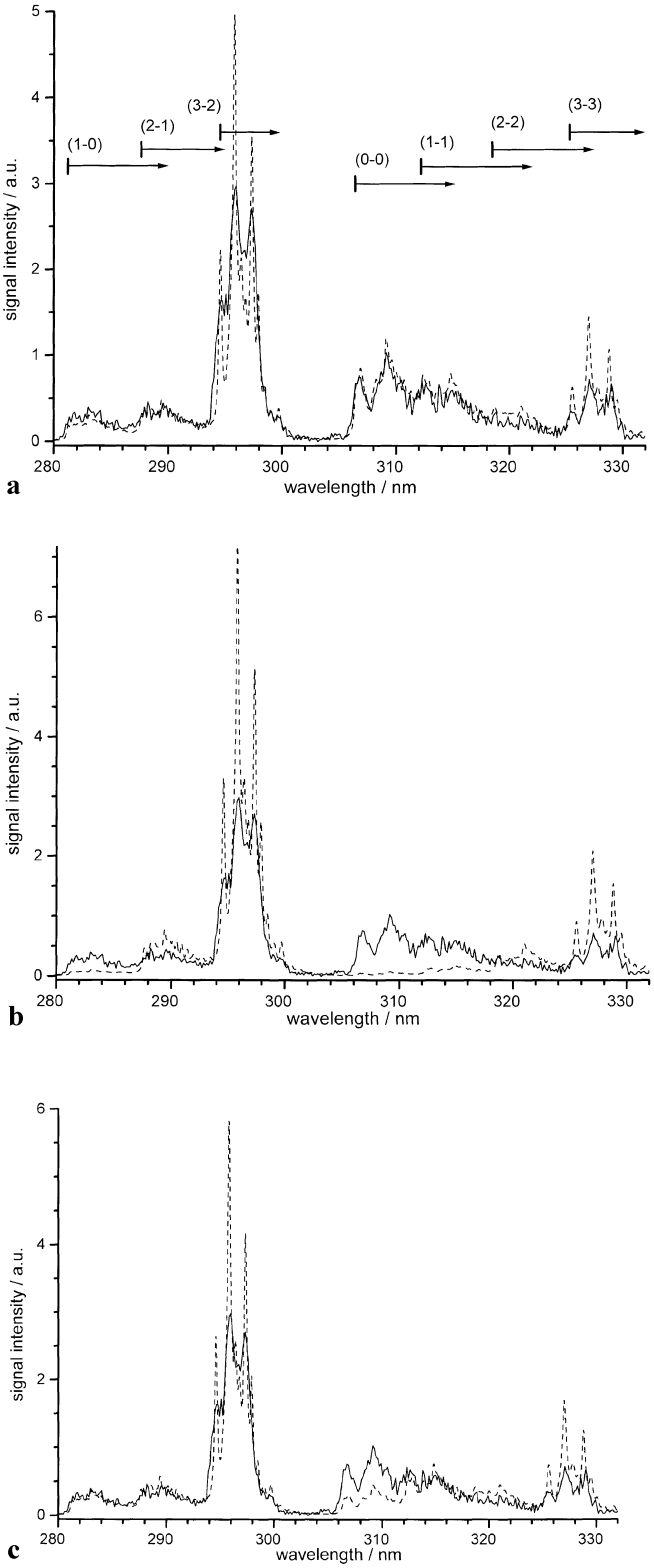

Fig. 3a–c. Experimental OH LIF spectrum [24] and simulations. *Full line*: spectrum measured in an atmospheric pressure CH_4/O_2 flame. Excitation: 3–0 band, $Q_1(4)$ line. Signal temporally integrated. *Broken line:* LASKIN simulations. **a** Shows the best agreement, found with the simulation parameters as described in the text and Table 1. Discrepancies in the 3–2 and 3–3 band amplitudes are ascribed to the effects of excitation with a polarized laser. **b** For this simulation only the vibrational deactivation channels with $\Delta v = 1$ were allowed. **c** The channels with $\Delta v = 1$ and $\Delta v = 2$ were allowed

laser-pumped level; hence the amplitudes of the most prominent lines are not well reproduced. Apart from that, the simulation can fairly well reproduce the general features of the experiment. It should be noted that for the $v' = 1$, 2, and 3 levels two vibrational bands, one each from the $\Delta v = 0$ and $\Delta v = 1$ progressions, are contained in the spectral range and have to be reproduced simultaneously. There are small discrepancies, for example in the 2–2 band region, that could be reduced by altering the relative velocities of VET, but only at the expense of deteriorating the agreement in the 2–1 band area. The vibrational bands also overlap to some degree, particularly in the $\Delta v = 0$ progression, and with the given experimental resolution it is difficult to accurately assign the contributions of different levels. It should be noted that the 3–2 and 3–3 bands are not perfectly free from spectral interference with the lower levels.

In further calculations for the same experimental spectrum, some of the assumptions made for the VET coefficients (see Table 1a) were tested in more detail by systematic variation of parameters. Figure 3b shows a simulation where vibrational relaxation was only permitted in $\Delta v = 1$ steps. The rate coefficients $k_i^{\text{VET, total}}$ were kept fixed at the values determined for $v' = 1 \rightarrow 0$ transfer. As can be seen, the population of $v' = 2$ is strongly overestimated, and the two lowest vibrational levels are lacking intensity. This can not even be remedied by increasing the VET rates for the $v' = 3 \rightarrow 2$ and $v' = 2 \rightarrow 1$ transitions by a factor of 2 and 1.5, respectively. The effect of permitting $\Delta v = 2$ steps is demonstrated in Fig. 3c. While a reasonable-looking agreement for the bands originating from $v' = 2$ and 1 is achievable, the 0–0 band clearly is too weak. This suggests that vibrational relaxation steps with $\Delta v = 2$ and $\Delta v = 3$ are important processes occuring at rates that are of roughly the same order of magnitude as the $v' = 1 \rightarrow 0$ VET transitions measured so far. Similar conclusions for vibrational relaxation from the $v' = 2$ level were already drawn in [38]. The analysis in [40] also comes to the conclusion that relaxation steps with $\Delta v = 2$ and 3 must play a role, but no definite statements could be made about the branching ratios between the various vibrational relaxation pathways.

As discussed above, the nascent rotational distribution after a vibrational relaxation step is not known. Therefore the effect of using a different assumption (the "$2J + 1$" model described above) was studied in the simulation shown in Fig. 4. Compared with the "equal probability" model employed in the simulations of Fig. 3, this "$2J + 1$" assumption leads to a population shift towards the higher rotational levels in the collision-populated vibrational state (see [10]). In the particular case shown, levels in $v' = 0$ up to $N' = 20$ are included in the calculations. Both quenching and RET proceeds more slowly in these higher rotational levels. As is shown in Fig. 4, the "$2J + 1$" model assumption produces a distinctly different spectral shape in the 0–0 band region and a slightly poorer overall agreement with the experiment. On the other hand, in the comparisons made in [10] the "$2J + 1$" assumption had been more successful for reproducing a different set of experimental spectra than the "equal probability" assumption (which is otherwise used throughout for the calculations shown here). As was already discussed in [10], both model assumptions must be regarded as rather crude, and lack a theoretical basis. Therefore it is felt that, in this respect, no recommendations can be derived from the rather small number of samples that we could analyze so far.

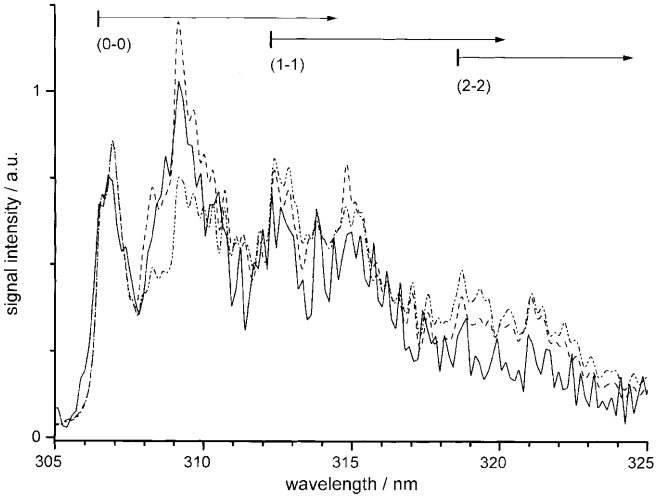

Fig. 4. A part of the same experimental spectrum as in Fig. 3 shown on an expanded wavelength scale. Two model assumptions regarding the nascent rotational distribution are compared: The "equal probability" assumption (*dashed line*) and the "$2J + 1$" assumption (*dash-dotted line*). Note the different spectral envelopes in the 0–0 band region near 308–310 nm

Other combinations of fuel and oxidizer provide different collider species in varying concentrations. Therefore simulations were also performed for spectra measured [24] in other flames. First, the spectrum from an atmospheric pressure H_2/O_2 flame ($T = 2000$ K) was calculated with the extended LASKIN code. Here, H_2O is the main collision partner with an 85% mole fraction. For the calculation the same set of coefficients was used that had led to the best agreement with the CH_4/O_2 flame spectrum shown in Fig. 3a. Figure 5a compares experiment and simulation for this H_2/O_2 flame. As can be expected from the poor VET efficiency of water, the signal stems mostly from the $v' = 3$ level. As in Fig. 3, effects due to laser polarization are clearly visible in the amplitudes of the prominent lines that originate from the directly laser-pumped level. For the signal from collision-populated levels, the agreement between simulation and experiment is reasonable.

As mentioned above, nitrogen is very inefficient as quencher, but possesses a relatively large cross section for VET; also, from a practical point of view, N_2 is important as a major species in air-fed combustion. Hence simulations were performed for a spectrum [24] measured in an atmospheric pressure methane–air flame ($T = 2050$ K). Figure 5b shows the comparison. Again, the amplitudes of lines from the laser-pumped level exhibit anomalous intensities due to polarization effects. But more important, the large percentage of N_2 present in the air-fed flame leads to a drastic change in the relative amplitudes of vibrational bands. The collision-populated levels are now responsible for about 70% of the signal [24]. As can be seen, the overall agreement between simulation and experiment is not as good as in the case of the CH_4/O_2 flame shown in Fig. 3a. In particular the 0–0 band intensity is overestimated, and the discrepancies in the 1–0 and 2–1 band regions are larger.

Finally, simulations of the ($OH + N_2$) system were made for a spectrum (Fig. 6) that was taken under very different experimental conditions [39]. OH was generated in a room-

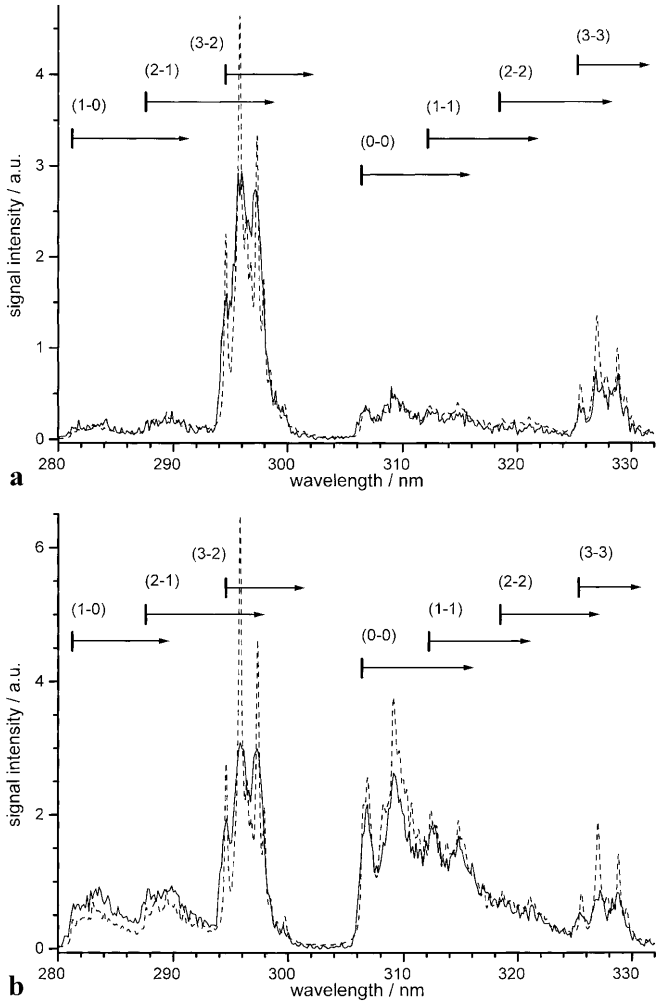

Fig. 5a,b. Experimental OH LIF spectra [24] and simulation. Excitation: 3–0 band, $Q_1(4)$ line. Signal temporally integrated. Discrepancies in the 3–2 and 3–3 band amplitudes are again ascribed to the effects of excitation with a polarized laser. **a** *Full line* is spectrum measured in an atmospheric pressure H_2/O_2 flame. *Broken line*: LASKIN simulation. **b** *Full line* is spectrum measured in an atmospheric pressure CH_4/air flame. *Broken line*: LASKIN simulation

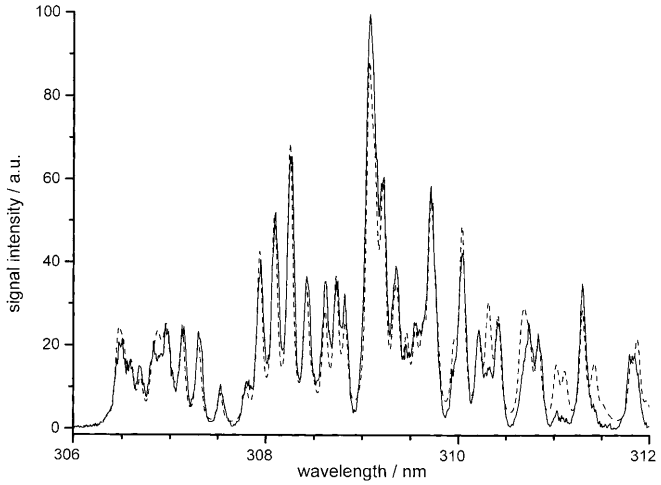

Fig. 6. *Full line*: Experimental OH LIF spectrum [39] from a low-pressure, room-temperature flow reactor. Total pressure: 0.92 Torr; partial pressure N_2: 0.23 Torr, with He as bath gas. Excitation: 1–0 band, $Q_1(2)$ line. Signal temporally integrated. *Broken line:* LASKIN simulation. Although agreement for the regime of low to medium rotational levels appears reasonably good, discrepancies are discernible for the higher levels. It should be noted that the simulation predicts strong signals e.g. around 311.1 nm ($Q_2(12)$, $Q_1(13)$ line), whereas the experiment shows only marginal intensities there

temperature He flow (0.69 Torr) doped with 0.23 Torr of nitrogen. Excitation was in the 1-0 band $Q_1(2)$ line, and the time-integrated emission was recorded in the 0–0 band. The simulation shown in Fig. 6 exhibits the general trends of the spectrum, but the populations of the higher rotational levels are overestimated. For several Q-branch lines, for example the $Q_2(12)$ and $Q_1(13)$ lines near 311.3 nm, intensities are predicted that are much larger than the experimental values. It may be assumed that these shortcomings are, to a large extent, attributable to the way the nascent rotational distribution after a VET step is handled by the "equal probability" model assumption [10] used here. In [39] analysis of other LIF spectra from the $OH + O_2$ and $OH + Ar$ systems resulted in apparently bimodal population distributions in $v' = 0$, an effect that could hardly be accounted for with these model assumptions.

The dependence of VET on the initially pumped rotational level could be investigated by using spectra from the CH_4/O_2 flame [40] where the $Q_1(8)$ and $Q_1(11)$ lines in the 3–0 band were excited. A calculation for the $Q_1(8)$ excitation line (not shown here), using parameters identical with those employed in Fig. 3a, produces a spectrum where the agreement with experiment is slightly worse in the 0–0 band region, but otherwise comparable with the case shown in Fig. 3a. In the spectrum excited via the $Q_1(11)$ line, the S/N ratio is not sufficient to draw valid conclusions. This decreased S/N is largely due to the further shortened predissociation lifetime of the $N' = 11$ rotational level (54 ps as compared to 250 ps for $N' = 4$), leading to much less population transfer to the lower vibrational states.

Additional simulations for the CH_4/O_2 flame [40] (also not depicted here) confirmed that the quenching rates assigned to $v' = 2$ and 3 do not have much influence on spectral shapes and amplitudes; setting the rate coefficients for all four vibrational levels equal to the $v' = 0$ value hardly affects the result.

3 Discussion

It may have become clear from the preceding paragraphs that detailed simulation of the collisional effects on OH LIF spectra requires an intimidatingly large number of input parameters. Some of them are well known, and some can be extrapolated or estimated in a reasonable way. However, there remains a large field for the simulator's intuition. This situation is perhaps analogous to the case of flame chemistry modeling, where many rate coefficients as well as their temperature and pressure dependence are poorly known.

The spectra originating from higher vibrational levels generally prove less sensitive to collisional effects, because these states have comparably short predissociative lifetimes. The exact magnitude of quenching rates for $v' = 2$ and 3 is therefore not too important an issue, at least for atmospheric and lower pressure. This was already implied in the early paper [11] dealing with LIF excitation to $v' = 3$. The RET does have a visible effect for $v' = 2$, and the rate coefficients that were measured for $v' = 0$ seem to provide a reasonably good

starting point for the description of RET in $v' = 2$ and 3. This agrees with a trend that was observed [35] in the comparison between measured coefficients for $v' = 0$ and $v' = 1$. In the rapidly predissociating $v' = 3$ state, RET has only a minor effect in terms of redistribution. An exact comparison with experimental data is particularly difficult for $v' = 2$ and 3 when polarized lasers are used in the experiment. A certain fraction (which is a priori unkown) of the resulting alignment will be preserved over several state-changing collisions [14, 16], thus affecting the relative signal intensities in the measured LIF spectrum. It seems as if the advantage of being insensitive to quenching collisions could be balanced by the additional problems associated with signal depolarization. First measurements of depolarization rates were reported [16, 42]. If a more thorough check of the assumptions regarding the RET rate coefficients in $v' = 2$ and 3 should become desirable, these details will also have to be addressed.

For the lower vibrational states, however, additional measurements of state-specific RET coefficients would be very helpful, particularly for the high rotational levels. These are not only important at flame temperatures, but may also become involved during vibrational relaxation. As mentioned above, the calculation of rate coefficients for collisions with N_2 and CO_2 is not yet as satisfactory as it is for water. Therefore, more data could be put to good use, both to reduce uncertainties implied in the ECS scaling law extrapolations into the high-temperature, high-J regime, and also for providing material to develop and test other models for the description of RET by these colliders. The use of lasers and detection equipment capable of time resolution on the ps scale [16–18, 43] should facilitate such measurements.

Vibrational relaxation from $v' = 3$ and $v' = 2$ is an important issue in the context of LIF measurements, because it will populate the longer-lived lower states which then fluoresce with a much higher quantum yield than the originally pumped predissociative level. While this will of course increase the signal levels, it also re-introduces questions about collisional effects for a quantitative analysis. Even if the spectral detection bandwidth is carefully matched to, for example, the 3–2 or 3–3 band, there may still be a certain amount of signal originating from high rotational levels in the $v' = 2$ state which overlaps this spectral range.

Quite generally, the experimental data base for vibrational relaxation effects is not yet satisfactory. The calculations presented here clearly suggest that up to three vibrational quanta may be transferred in a single collision, confirming a trend that was observed in earlier work [24, 38]. Cross sections for the processes with step sizes $\Delta v = 1$, 2, and 3 seem to be of a similar order of magnitude. However, important details are still unknown. The branching ratio between these relaxation pathways has not yet been established for the simplest flame, let alone for a well-defined single collider species. The dependence on vibrational and rotational level, temperature and collider species are further questions awaiting clarification. Experimental VET coefficients for the upper vibrational levels are needed. From a practical point of view, the behaviour of nitrogen and CO_2 will be particularly important to know because of their large VET cross sections and abundance in air-fed combustion. Systems using rare gases as colliders may be more accessible for ab initio calculations, as was the case for the investigation of RET processes [44, 45].

Even less is known about the nascent rotational distribution after the VET step, which forms the starting point for rotational relaxation within the collisionally populated level. From previous work [10, 38, 39] it is known that rather wide rotational distributions are obtained which also show features specific to the collider. This point is not yet well understood. The simple model assumptions [10] that were used here for describing this behaviour can not be regarded as satisfactory. None of them yields a consistently good agreement with experiment for all conditions that were employed in [10] and in this work. In particular, these models would hardly be able to reproduce the apparently bimodal rotational distributions that were observed [39] after the $v' = 1 \rightarrow 0$ VET step for collisions of OH with oxygen and OH with argon.

It has been repeatedly stated that the modeler suffers from a lack of "hard data", the more so, the higher the energy is of the levels considered. Another problem with comparisons to literature spectra lies in the frequent lack of some important experimental parameters in the description. It should have become obvious from the discussion in the preceding paragraphs that a fairly detailed knowledge of flame composition, temperature, pressure, as well as laser and detection parameters is required for a simulation. Incompleteness of specifications does quite severely limit the number of spectra that are available for simulation purposes. But even though a very substantial fraction of the rate coefficients employed in this work are not much more than the result of an educated guess, a fair degree of agreement between calculation and experiment is achieved with a consistent set of parameters for widely varying experimental conditions. This may permit the conclusion that the simulation model described here, while there is undoubtedly much room for improvement of many important details, conveys a surprisingly reasonable picture of some general tendencies observable in the OH relaxation behaviour in flames.

Although the main focus of the present study was the investigation of the collisional dynamics in OH LIF experiments, the question may be permitted which implications the obvious lack of precise energy transfer data for some of the conditions analyzed here has for typical LIF experiments using ns pulse lasers. There is no general answer in terms of the "typical" accuracy or precision attainable in OH concentration measurements, or in temperature measurements using OH as an indicator. The achievable result depends, to a large extent, on the experimental procedure and the collisional environment, and many approaches have been discussed in the literature. Linear OH LIF using ns lasers and detection equipment have been successfully applied under various flame conditions, and concentration measurements with an accuracy of about 10%–20% have been demonstrated. Also, temperatures have been determined with an error limit of about 100 K at 2000 K. While this may be achievable under conditions with good signal-to-noise ratio, low background emission, negligible laser or signal absorption and a well-known collisional environment, accurate measurements may be more challenging, for example, in large devices, at very low or high pressures, or in fuel-rich and sooting flames. Also, the accuracy of single-pulse two-line temperature field measurements in turbulent combustion may still prove unsatisfactory. If the effect of collisional energy transfer cannot be estimated, it is often wise to rely on calibration measurements in a well-known combustion environment, or on a cross-

check with a different diagnostic technique under selected conditions.

Acknowledgements. We thank T. Nielsen, F. Bormann, K. Steffens, and L. Williams for kindly providing us with data files of their experimental spectra, as well as P. Andresen and the OSA for their kind permission to reproduce Fig. 2a. We thank one of the referees for bringing our attention to a reference [36]. The authors acknowledge financial support by the DFG under contract Ko1363/9-1.

References

1. A. Arnold, A. Bräumer, A. Buschmann, M. Decker, F. Dinkelacker, T. Heitzmann, A. Orth, M. Schäfer, V. Sick, J. Wolfrum: Ber. Bunsenges. Phys. Chem. **97**, 1650 (1993)
2. K. Kohse-Höinghaus: Prog. Energy Combust. Sci. **20**, 203 (1994)
3. J.L. Palmer, R.K. Hanson: Appl. Opt. **35**, 485 (1996)
4. J.W. Daily: Prog. Energy Combust. Sci. **23**, 133 (1997)
5. E.W. Rothe, P. Andresen: Appl. Opt. **36**, 3971 (1997)
6. C. Chan, J.W. Daily: Appl. Opt. **19**, 1357 (1980)
7. D.H. Campbell: Appl. Opt. **23**, 689 (1984)
8. R.P. Lucht, D. Sweeney, N.M. Laurendeau: Appl. Opt. **25**, 4086 (1986)
9. R. Kienle, M.P. Lee, K. Kohse-Höinghaus: Appl. Phys. B **62**, 583 (1996)
10. A.T. Hartlieb, D. Markus, W. Kreutner, K. Kohse-Höinghaus: Appl. Phys. B **65**, 81 (1997)
11. P. Andresen, A. Bath, W. Gröger, H.W. Lülf, G. Meijer, J.J. ter Meulen: Appl. Opt. **27**, 365 (1988)
12. J.A. Gray, R.L. Farrow: J. Chem. Phys. **95**, 7054 (1991)
13. D.E. Heard, D.R. Crosley, J.B. Jeffries, G.P. Smith, A. Hirano: J. Chem. Phys. **96**, 4366 (1992)
14. P.M. Doherty, D.R. Crosley: Appl. Opt. **23**, 713 (1984)
15. E.W. Rothe, Y.-W. Gu, G.P. Reck: Appl. Opt. **35**, 934 (1996)
16. P. Beaud, P.P. Radi, D. Franzke, H.-M. Frey, B. Mischler, A.-P. Tzannis, T. Gerber: Appl. Opt. **37**, 3354 (1998)
17. F.C. Bormann, T. Nielsen, M. Burrows, P. Andresen: Appl. Opt. **36**, 6129 (1997)
18. T. Nielsen, F. Bormann, M. Burrows, P. Andresen: Appl. Opt. **36**, 7960 (1997)
19. W. Ketterle, M. Schäfer, A. Arnold, J. Wolfrum: Appl. Phys. B **54**, 109 (1992)
20. G.-S. Kim, H. An, E.W. Rothe, L.M. Hitchcock, Y. Gu, G.P. Reck: SPIE Proc. **1862**, 154 (1993)
21. J.M. Seitzman, R.K. Hanson: AIAA J. **31**, 513 (1993)
22. T.M. Quagliaroli, G. Laufer, J.C. McDaniel: Appl. Phys. B **59**, 635 (1994)
23. G. Laufer, T.M. Quagliaroli, R.H. Krauss, R.B. Whitehurst III, J.C. McDaniel, J.H. Grinstead: AIAA J. **34**, 463 (1996)
24. K.L. Steffens, J.B. Jeffries, D.R. Crosley: Opt. Lett. **18**, 1355 (1993)
25. K. Kohse-Höinghaus, J.B. Jeffries, R.A. Copeland, G.P. Smith, D.R. Crosley: 22nd Symposium (International) on Combustion, The Combustion Institute, Pittsburgh, USA, 1988, pp. 1857–1866 **1857**, (1988)
26. R. Kienle, M.P. Lee, K. Kohse-Höinghaus: Appl. Phys. B **63**, 403 (1996)
27. A.E. DePristo, S.D. Augustin, R. Ramaswamy, H. Rabitz: J. Chem. Phys. **71**, 850 (1979)
28. P. Monkhouse, S. Selle: Appl. Phys. B **66**, 645 (1998)
29. P.H. Paul: J. Quant. Spectrosc. Radiat. Transfer **51**, 511 (1994)
30. P. Deuflhard, P. Bader, U. Nowak: In *Modeling of Chemical Reaction Systems*, ed. by K.H. Ebert, P. Deuflhard, W. Jaeger (Springer Ser. Chem. Phys. **18**, 38 (1981)
31. J. Luque, D.R. Crosley: *LIFBASE: Database and Spectral Simulation Program (Version 1.1)* SRI International Report MP **96-001** (1996)
32. D.R. Yarkony: J. Chem. Phys. **97**, 1838 (1992)
33. Q.-V. Nguyen, P.H. Paul: Appl. Opt. **36**, 2675 (1997)
34. E.W. Rothe, Y. Gu, A. Chryssostomou, P. Andresen, F. Bormann: Appl. Phys. B **66**, 251 (1998)
35. R. Kienle, A. Jörg, K. Kohse-Höinghaus: Appl. Phys. B **56**, 249 (1993)
36. K.W. Holtzclaw, B.L. Upschulte, G.E. Caledonia, J.F. Cronin, B.D. Green, S.J. Lipson, W.A.M. Blumberg, J.A. Dodd: J. Geophys. Res. **102**, 4521 (1997)
37. P.H. Paul: J. Phys. Chem. **99**, 8472 (1995)
38. R.K. Lengel, D.R. Crosley: J. Chem. Phys. **68**, 5309 (1978)
39. L.R. Williams, D.R. Crosley: J. Chem. Phys. **104**, 6507 (1996)
40. K.L. Steffens: Ph.D. Dissertation, Stanford University (1994)
41. R.A. Copeland, M.L. Wise, D.R. Crosley: J. Phys. Chem. **92**, 5710 (1988)
42. A. Dreizler, R. Tadday, A.A. Suvernev, M. Himmelhaus, T. Dreier, P. Foggi: Chem. Phys. Lett. **240**, 315 (1995)
43. M. Köllner, P. Monkhouse, J. Wolfrum: Chem. Phys. Lett. **168**, 355 (1990)
44. A. d'Esposti, H.-J. Werner: J. Chem. Phys. **93**, 3351 (1990)
45. A. Jörg, A. d'Esposti, H.-J. Werner: J. Chem. Phys. **93**, 8757 (1990)